


UCRL- 84336
PREPRINT

PROFILE MODIFICATION AND HOT ELECTRON
TEMPERATURE FROM RESONANT ABSORPTION
AT MODEST INTENSITY

J. R. ALBRITTON
A. B. LANGDON

This paper was prepared for submittal
to American Physical Society Twenty-
Second Annual Meeting held in San Diego,
California, November 10 - 14, 1980.

October 13, 1980



Lawrence
Livermore
Laboratory

This is a preprint of a paper intended for publication in a journal or proceedings. Since changes may be made before publication, this preprint is made available with the understanding that it will not be cited or reproduced without the permission of the author.

CIRCULATION COPY
SUBJECT TO RECALL
IN 300 WEEKS

DISCLAIMER

This document was prepared as an account of work sponsored by an agency of the United States Government. Neither the United States Government nor the University of California nor any of their employees, makes any warranty, express or implied, or assumes any legal liability or responsibility for the accuracy, completeness, or usefulness of any information, apparatus, product, or process disclosed, or represents that its use would not infringe privately owned rights. Reference herein to any specific commercial products, process, or service by trade name, trademark, manufacturer, or otherwise, does not necessarily constitute or imply its endorsement recommendation, or favoring of the United States Government or the University of California. The views and opinions of authors expressed herein do not necessarily state or reflect those of the United States Government or the University of California, and shall not be used for advertising or product endorsement purposes.

Profile Modification and Hot Electron
Temperature from Resonant Absorption
at Modest Intensity

J. R. Albritton and A. B. Langdon
University of California, Lawrence Livermore Laboratory.
Livermore, California 94550

ABSTRACT

Resonant absorption is investigated in expanding plasmas. The momentum deposition associated with the ejection of hot electrons toward low density via wavebreaking readily exceeds that of the incident laser radiation and results in significant modification of the density profile at critical. New scaling of hot electron temperature with laser and plasma parameters is presented.

*Work performed under the auspices of the U.S. Department of Energy by the Lawrence Livermore Laboratory under contract number W-7405-ENG-48.

Theory indicates that lasers of current application may be expected to exhibit significant collisionless interaction with inertial confinement fusion targets. Here we consider resonant absorption¹ which acts at critical density where the laser frequency equals the local electron plasma frequency. Because the dominant laser-plasma coupling occurs near critical it is essential to develop a self-consistent description of the dynamics there. It will be seen that even weak resonant absorption acts strongly upon the hydrodynamical evolution of this region so as to enhance itself and suppress other mechanisms.

Resonant electron oscillations transfer absorbed energy to the plasma by ejecting particles toward low density via wavebreaking.¹ The associated momentum deposition readily exceeds that of the driving laser radiation. These hot collisionless electrons are confined by the electrostatic potential and subsequently pose two challenges to laser fusion: 1). to prevent them from preheating the target and 2). to use their energy to drive its implosion.

Implosion experiments at modest intensity are already in progress² to increase the density of the compressed core above that of high intensity exploding pusher target experiments³ which are strongly preheated by hot electrons from resonant absorption. The scaling of hot electron temperature in the high intensity regime is the subject of recent theoretical work;^{4,5} briefly, the laser

beam or driven wave steepens the density profile at critical and thereby reduces the rate of increase of the hot electron temperature with increasing laser intensity from estimates based on the usual coronal rarefaction .

Here we report new and improved scaling laws for the temperature of hot electrons produced by resonant absorption in the modest intensity regime. (We will, in fact, argue for the general validity of our results). The dependence of hot electron temperature upon background cold electron temperature is shown to be as strong as that upon laser intensity.

The interaction of modest intensity $1.06\text{ }\mu\text{m}$ laser radiation with high Z disc targets has been modeled by ad hoc strong limitation of electron energy conduction.⁶ The resulting coronal rarefaction exhibits a step in density including critical and hot plasma below the subcritical density at which the flow emerges from the step. Most interaction mechanisms are suppressed in such a profile.

In fact resonant absorption is enhanced in a self-consistent stepped density profile^{1,4,5,7}. Here we provide a first principles model of profile modification in the modest intensity regime as the local response of the flow to the momentum deposited at critical by hot electron production. The efficiency of coupling hot electron energy from the corona to drive the compression of the core is a subject of current research.⁸

The upper density of the induced step may be much greater than critical and much greater than that associated with radiation

pressure steepening. Experimental observations of such structures have been reported recently.⁹ The associated lower density and absence of an extensive turning region act to suppress inverse bremsstrahlung and stimulated Brillouin scattering. The step in electrostatic potential associated with the density step contributes to the formation of a hot corona since electrons sufficiently energetic to climb it may be expected to possess an elevated temperature as well.

Here we present a summary of results and their interpretation of a study performed with the one dimensional electrostatic particle simulation code ESI¹⁰ to investigate the scaling of energy, momentum and charge balance of resonant absorption in the modest intensity regime. We define the modest intensity regime to be that in which the driven wave pressure dominates the laser radiation pressure. Our neglect of electromagnetism is then justified as the laser is seen to contribute primarily energy to the system while in the high intensity regime it contributes both energy and momentum.

The physical notion which motivates our work and guides our analysis is that the system relaxes locally to a quasi-steady equilibrium in which the sharply peaked energy density or ponderomotive pressure of the resonant wave is balanced on the overdense side by the background plasma pressure and on the underdense side by the reaction to the momentum flux of hot electrons ejected toward the vacuum. The critical density region and driven resonant wave is shown in Fig. 1.

From consideration of pressure balance on the underdense side of the wave we estimate, $E^2/8\pi \sim (\pi/2)^{1/2} f I/v_h$.¹¹ Here f is the absorption fraction of laser intensity I into hot electrons of velocity $v_h = (T_h/m)^{1/2}$.

The momentum flux of hot electrons exceeds that of the laser radiation whenever $(\pi/2)^{1/2} f I/v_h > (2 - f) I/c$ or

$$T_{h, \text{modest}} < (511 \pi/2) f^2/(2 - f)^2 \text{ keV} \quad (1)$$

Experience indicates that 0.3 is a useful estimate for f ; Eq. (1) then becomes $T_{h, \text{modest}} < 25 \text{ keV}$, and the modest intensity regime in the laboratory is found to be,¹² $I(\text{W/cm}^2) \lambda^2 (\mu)|_{\text{modest}} < 10^{16}$.

Momentum balance on the overdense side of critical is established by the background cold electron pressure and the wave pressure. Thus $-\nabla(N T_c) \sim -\nabla(E^2/8\pi) \sim -\nabla(\pi/2)^{1/2} f I/v_h$ so that by crude integration the upper density associated with resonant absorption, N_u^* , is estimated to be,

$$N_u^*/N_c \sim 1 + (\pi/2)^{1/2} f I/N_c T_c v_h \quad (2)$$

For the experimental parameters of Ref. 10 this steepening is more than three times that associated with the radiation pressure!

In general the radiation pressure contribution should be included in estimating the upper density. However, an upper density greater than that given in Eq. (2) may be expected not to change the dynamics of the driven resonant wave qualitatively from that described here. The longer scalelength ($\sim c/\omega_p$) over which the radiation pressure acts suggests a doubly stepped profile in which the resonant wave dominates locally but where the maximum density may be determined by radiation pressure. In this picture our results may be extended to the high intensity regime.

Our simulation code evolves the dynamics of an initially uniform slab of electrons and ions which expand into vacuum under the influence of a high frequency capacitor model¹ pump. The pump frequency is chosen well below the plasma frequency of the initial slab. By mapping the hot electron heating rate onto absorbed laser intensity¹ we will cast our results into a form useful for laboratory application¹² and comparison to electromagnetic simulations^{1,4,5}.

The driven systems are characterized by the single dimensionless parameter, v_0/v_c ($T_e/T_i \sim 3$, $m/M \sim 1/900$). This is the ratio of the jitter velocity of an electron oscillating freely in the pump field, $v_0 = eE_0/m\omega_0$, and the initial (cold) electron thermal velocity, $v_c = (T_c/m)^{1/2}$. The space and time scales of the rarefaction and resonant wave are determined self-consistently.

Our principal results are the variation with v_0/v_c of the

hot electron temperature, the hot electron heating rate, and the densities delimiting the step. In general the stepped density profile dominates our results and, while not a failure for certain purposes, a description of the system in terms of a single scalelength is not appropriate. Even for v_o/v_c less than $(m/M)^{1/2}$ we find that wavebreaking governs the system: neither convection nor soliton formation have been seen.

In Fig. 2, the normalized hot electron temperature, T_h/T_c , and the normalized hot electron heating rate, $Q_h/N_c T_c v_c$, are plotted against v_o/v_c . Note the break in the data at $v_o/v_c \sim 1$. Cold plasma modeling is appropriate for $v_o/v_c > 1$ while $v_o/v_c < 1$ is the warm plasma regime.

Let us now identify the hot electron heating rate with absorbed laser intensity. We have $Q_h/N_c T_c v_c$ and T_h/T_c as functions of v_o/v_c ; we identify $Q_h = fI$ and then eliminate v_o/v_c to obtain the data displayed in Fig. 4. Note the role played by the background temperature as T_h/T_c varies against $fI(W/cm^2)\lambda^2(\mu)/T_c^{3/2}(ev)$. The break in the scaling is clearly evident. In the warm plasma limit $fI\lambda^2/T_c^{3/2} < 10^{11}$ we have drawn lines with slopes of 2/5 and 1/3. These yield the preferred scaling, $T_h(ev) = 9 \times 10^{-4} (fI\lambda^2 T_c)^{2/5}$, which compares favorably with that given in Ref. 5, and still within confidence limits, $T_h = 4 \times 10^{-3} (fI\lambda^2)^{1/3} T_c^{1/2}$, which compares favorably with that given in Ref. 4. Note that the scaling with cold background temperature is as strong as that with

intensity. The cold plasma limit given in Ref. 13 is recovered for $fI\lambda^2/T_c^{3/2} > 10^{11}$, where $T_h = 9 \times 10^{-7}(fI\lambda^2)^{2/3}$ independent of T_c .

Our results may be employed to gain information about the cold electron temperature from observation of the hot electron temperature. Comparison with the data of Giovanelli¹² suggests that the interaction in the laboratory is governed by cold plasma dynamics for $I\lambda^2 < 10^{15}$ where the 2/3 power obtains ($T_h/T_c =$ constant leads to the same scaling) and warm plasma dynamics for $I\lambda^2 > 10^{15}$ where the 2/5 or 1/3 power obtains. These considerations further suggest a change in the background plasma heating for $I\lambda^2 \sim 10^{15}$.

The 2/3 power scaling of hot electron temperature was suggested previously by flux limit and stochastic heating estimates¹⁴. Let us briefly recapitulate the cold plasma estimates for resonant absorption which yield the 2/3 power scaling¹³ confirmed here. Wavebreaking occurs when electrons oscillate in the wave with a velocity, $v_e \sim eE/m\omega$, which scales with the effective phase velocity of the wave $v_e \propto v_p \sim L/(2\pi/\omega)$. The hot electron temperature scales with the energy an electron can gain in riding the wave across the resonant region, $T_h \propto eEL$. Combining these we find $E^2/8\pi \sim N_c T_h/4\pi$. Recall that momentum balance on the underdense side of the wave requires $E^2/8\pi \sim (\pi/2)^{1/2} fI/v_h$. Combining again yields $T_h \propto (fI\lambda^2)^{2/3}$, exactly the desired result.

Finally in Fig. 4 we show the relative upper and lower densities bounding the step at critical, N_u/N_c and N_L/N_c respectively, as functions of $fI\lambda^2/T_c^{3/2}$. The estimated upper density, N_u^*/N_c from Eq. (2), is also plotted. The width of the step region decreases from some 25 local (cold) Debye lengths at $fI\lambda^2/T_c^{3/2} \sim 10^9$ to about 1 as $fI\lambda^2/T_c^{3/2}$ exceeds 10^{11} . The agreement of the estimated upper density is quite good except for the strongest pumps - neglect of the flow contribution to momentum balance in the step region^{1,7} may be the major source of error. Typical values of the lower density are seen to be less than half critical.

We gratefully acknowledge E. I. Thorsos, E. A. Williams and W. L. Kruer for their contributions to this work.

References

1. J. P. Friedberg, R. W. Mitchell, R. L. Morse, and L. I. Rudstinski; Phys. Rev. Lett. 28 795 (1972); P. Koch and J. Albritton Phys. Rev. Lett. 32, 1420 (1974) and Phys. Fluids 18 1136 (1975); K. Estabrook, E. J. Valeo and W. L. Kruer, Phys. Lett. 49A, 109 (1974) and Phys. Fluids 18, 1151 (1975); J. S. DeGroot and J. E. Tull, Phys. Fluids 18, 672 (1975). D.W. Forslund, J.M. Kindel, K. Lee, E.L. Lindman, and R.L. Morse; Phys. Rev. A, 11, 679 (1975).
2. W. C. Mead, et al., UCRL - 813163 (1979).
3. W. C. Mead, et al., UCRL-80006 (1977).
4. D. W. Forslund, J. M. Kindel and K. Lee, Phys. Rev. Lett. 39, 284 (1977).
5. K. Estabrook and W. L. Kruer, Phys. Rev. Lett. 40, 42 (1978).
6. M. D. Rosen, et al., Phys. Fluids 22, 2020, (1979).
7. D. W. Forslund, J. M. Kindel, K. Lee and E. L. Lindman, Phys. Rev. Lett. 36, 35 (1976).
8. J. R. Albritton, I. B. Bernstein, E. J. Valeo and E. A. Williams, Phys. Rev. Lett. 39, 1536 (1977).
9. R. Fedosejevs, M. D. J. Burgess, G. D. Enright and M. C. Richardson, Phys. Rev. Lett. 43, 1664, (1979).
10. C. K. Birdsall and A. B. Langdon, Plasma Physics via Computer Simulation, University of California Press, Berkeley (1975).
11. The factor $(\pi/2)^{1/2}$ results from employing a half Maxwellian distribution in computing the hot electron momentum flux in terms of its energy flux.
12. D. V. Giovanelli, LA-UR 76-2242 (1976); K. R. Manes et al., J. Opt. Soc. Am., 67, 717 (1977).

13. J. R. Albritton, E. I. Thorsos and E. A. Williams, LLE Rept. No. 85 (1978).
14. R. L. Morse and C. W. Nielson, Phys. Fluids 16, 909 (1973).

Figure Captions

1. In the critical density region the driven resonant wave supports itself against the background plasma pressure on the overdense side by the reaction pressure associated with the momentum flux of hot electrons ejected toward the underdense side. The curves are simulation data for $v_o/v_c = 1$ at $t = 1200/\omega_o$; $\omega_o = \omega_{p,max}/5$.
2. The hot electron temperature, T_h , and the hot electron heating rate, Q_h , increase with increasing pump strength, v_o . Note the break in the scaling at $v_o/v_c \sim 1$ which separates the regimes of warm plasma dynamics, $v_o/v_c < 1$, and cold plasma dynamics, $v_o/v_c > 1$. The two points plotted at $v_o/v_c = 1$ are runs of the same physical system with different pump frequencies. The difference in results there represents the uncertainty of our results throughout.
3. Identifying the hot electron heating rate, Q_h , with absorbed laser intensity, fI , the two curves in Fig. 2 are combined to obtain the scaling of the hot electron temperature with the laboratory observables f , $I(W/cm^2)$, $\lambda^2 (\mu)$, and $T_c(ev)$. Curve 1, with slope 2/5, curve 2 with slope 1/3, and curve 3, with slope 2/3, are discussed in the text.
4. The upper, N_u , and lower, N_L , densities delimiting the step at critical density, N_c , increase and decrease respectively with increasing effective pump strength. The estimated upper density, N_u^* of Eq. (2), is in agreement with observations except in the most strongly driven systems.

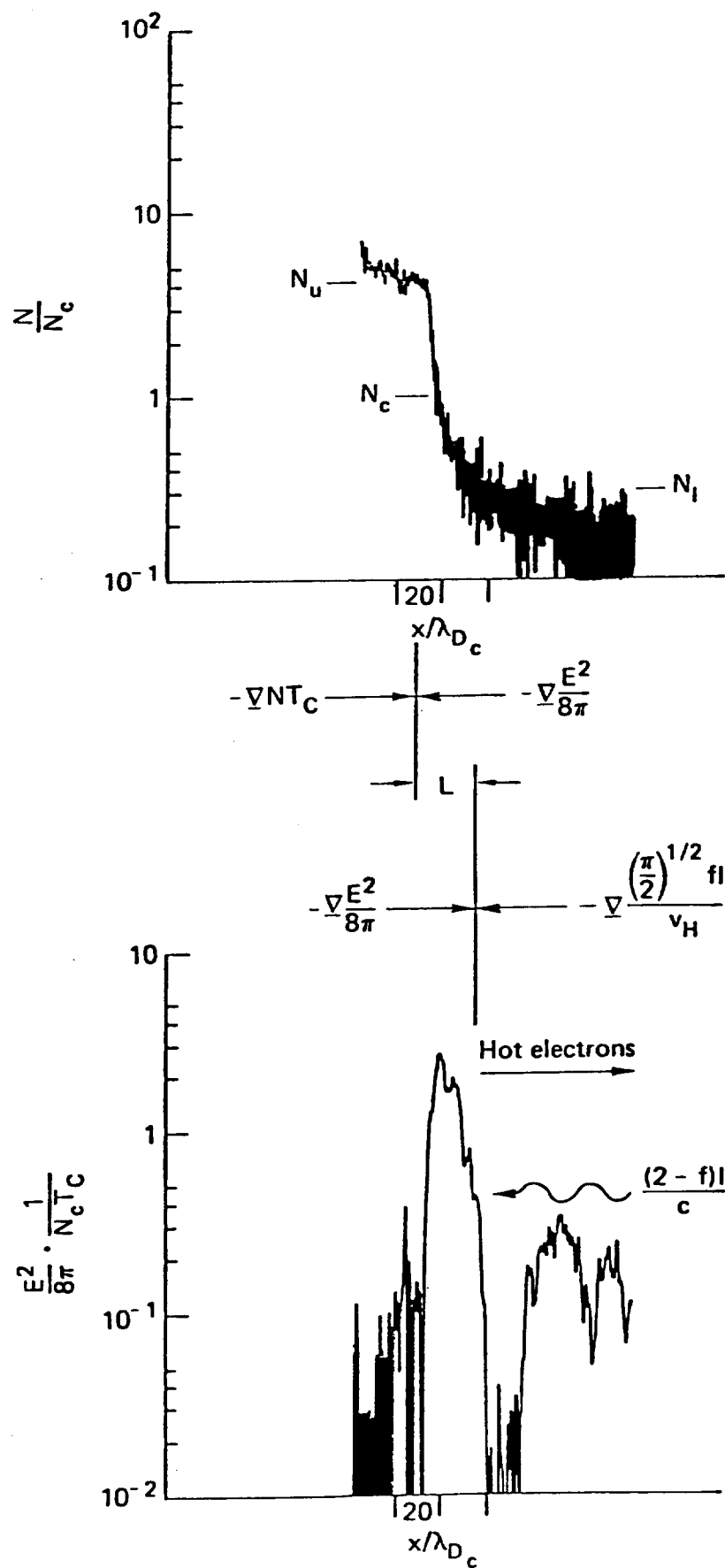


Figure 1

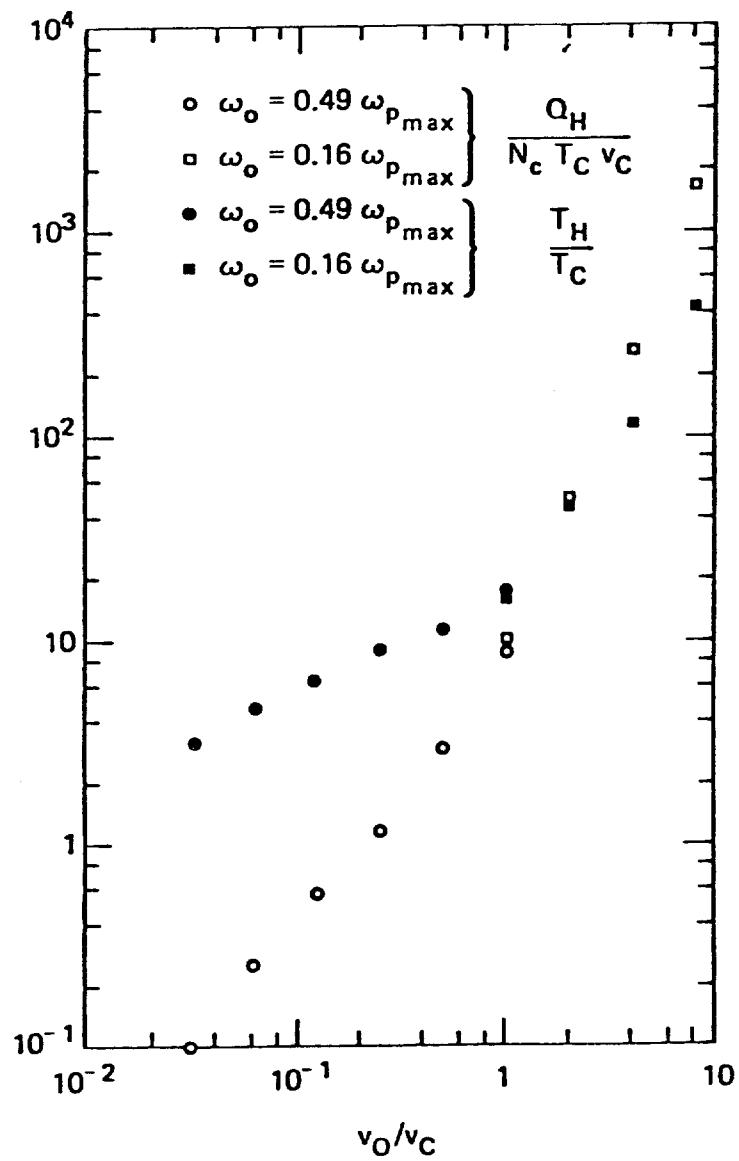


Figure 2

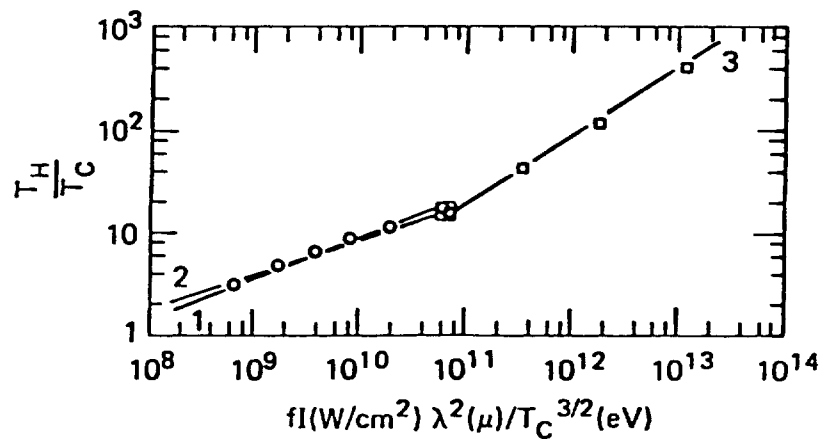


Figure 3

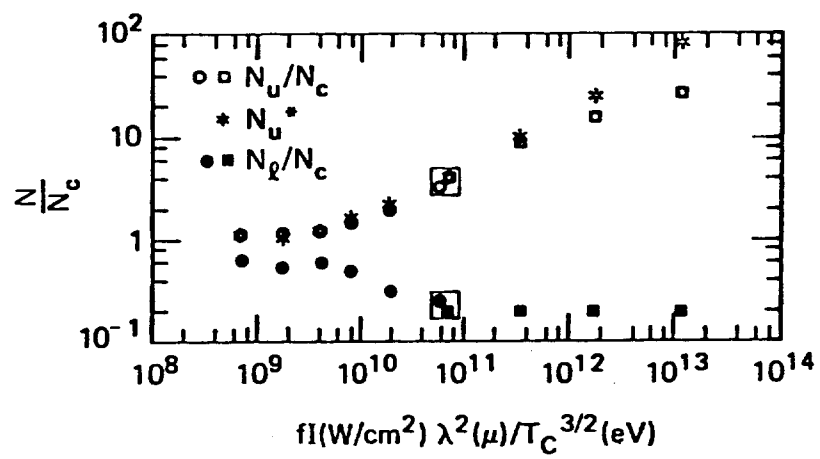


Figure 4